Iron oxide dissolution and solubility in the presence of siderophores

Originally published in:
Aquatic Sciences 66(1), https://doi.org/10.1007/s00027-003-0690-5

Aquat. Sci. 66 (2004) 3–18
1015-1621/04/010003-16
DOI 10.1007/s00027-003-0690-5

Aquatic Sciences

Review Article

Iron oxide dissolution and solubility in the presence of siderophores

Stephan M. Kraemer

Institute of Terrestrial Ecology, Swiss Federal Institute of Technology, Grabenstrasse 3, CH-8952 Schlieren, Switzerland

Received: 22 May 2003; revised manuscript accepted: 16 September 2003

Abstract. Iron is an essential trace nutrient for most known organisms. The iron availability is limited by the solubility and the slow dissolution kinetics of iron-bearing mineral phases, particularly in pH neutral or alkaline environments such as carbonatic soils and ocean water. Bacteria, fungi, and plants have evolved iron acquisition systems to increase the bioavailability of iron in such environments. A particularly efficient iron acquisition system involves the solubilization of iron by siderophores. Siderophores are biogenic chelators with high affinity and specificity for iron complexation.

This review focuses on the geochemical aspects of biological iron acquisition. The significance of iron-bearing minerals as nutrient source for siderophore-promoted iron acquisition has been confirmed in microbial culture studies. Due to the extraordinary thermodynamic stability of soluble siderophore-iron complexes, siderophores have a pronounced effect on the solubility of iron oxides over a wide pH range. Very small concentrations of free siderophores in solution have a large effect on the solution saturation state of iron oxides. This siderophore induced disequilibrium can drive dissolution mechanisms such as proton-promoted or ligand-promoted iron oxide dissolution. The adsorption of siderophores to oxide surfaces also induces a direct siderophore-promoted surface-controlled dissolution mechanism. The efficiency of siderophores for increasing the solubility and dissolution kinetics of iron oxides are compared to other natural and anthropogenic ligands.

Key words. Bioavailability; dissolution kinetics; iron acquisition; marine chemistry; plant nutrition; surface complexation.

Introduction

Iron is a micronutrient that is essential for a range of important enzymatic processes in most organisms. The consequences of iron deficiency are well documented and range from agricultural losses due to plant iron deficiency (Roemheld and Marschner, 1986) to the limitation of productivity in marine "High Nutrient Low Chlorophyll" (HNLC) regions (Martin and Fitzwater, 1988).

In most environments iron deficiency is not triggered by low total iron concentrations but by low iron bioavailability. For example, iron deficiency in plants is a widespread problem even though iron, in the form of iron-bearing minerals, is a ubiquitous component of the soil matrix. Similarly, in marine HNLC regions, which are characterized by very low total iron concentrations, only a fraction of the iron input by atmospheric aerosol is solubilized before sedimentation (Fung et al., 2000; Zhuang et al., 1990). An important limiting factor of iron bioavailability is the low solubility and slow dissolution kinetics of iron-bearing minerals.

To overcome these limitations, bacteria, fungi, and graminaceous plants (grasses) are known to sequester iron using siderophores (Neilands, 1957; Takagi, 1976; Winkelmann, 1992). Siderophores are low molecular weight organic ligands with high affinity and specificity

* Corresponding author phone: +41-1-633-6077;
fax: +41-1-633-1118; e-mail: kraemer@env.ethz.ch
Published on Web: March 24, 2004

for iron binding. The high affinity iron acquisition system is induced under iron limiting conditions and involves several steps (Boukhalfa and Crumbliss, 2002, and references therein):

- intracellular biosynthesis of siderophores
- exudation of siderophores in the extracellular space
- iron mobilization by competitive complexation or dissolution of iron-bearing minerals
- recognition and uptake of ferric siderophore complexes by highly efficient transport systems or liberation of iron from the siderophore complex and uptake of iron.

The details of molecular control of iron acquisition as well as the design of uptake systems are subject of active research. Siderophore production as a response to iron limitation is widespread among aerobic microorganisms (Neilands et al., 1987). For example, among 302 different fluorescent *Pseudomonas* strains isolated from soils, 297 strains (98%) produced detectable siderophores under iron stress (Cocozza and Ercolani, 1997). The ability to produce and assimilate siderophores with high affinities for iron(III) gives a microorganism an important selective advantage under iron-limited conditions.

Important prerequisites for the efficiency of this iron acquisition system are its affinity and specificity for Fe(III). The 1:1 stability constants of Fe(III) siderophore complexes are between 10^{23} and 10^{52} (Albrecht-Gary and Crumbliss, 1998; Ams et al., 2002) compared to 10^{20} for the iron(III)EDTA complex (Martell et al., 1995). The selectivity of the acquisition system for Fe(III) over similar ions such as Al(III) and ions that are often present in much higher concentrations such as Ca(II) is accomplished on two levels: by preferential chelation of Fe(III) and by recognition of the Fe(III) complex at receptor proteins at the cell surface. Preferential chelation of Fe(III) is an intriguing characteristic of siderophores. For example, the Fe(III) complex of the trihydroxamate siderophore desferrioxamine-B (DFO-B, see Fig. 1) has a 1:1 stability constant of $10^{30.6}$. This is many orders of magnitude higher then the corresponding Al(III) complex ($K = 10^{24.1}$) or the Ca(II) complex ($K = 10^{2.64}$) ($I = 0.1$, Smith et al., 2001). It should be noted that despite their high preference for Fe(III), the stabilities of many non-iron siderophore complexes are significant. Siderophores will therefore mainly exist in complexed form in most environmental systems.

As indicated above, a key function of siderophores is to sequester iron from the various iron pools that may be present in the particular environment in which the organisms are living. Important iron pools in soils and aquatic environments are iron complexes including ferric complexes with other ligands (including siderophores originating from other organisms); iron bound in enzymes etc. from lysing plant and microbial cells (recycling); iron bound to humic and fulvic substances; and iron-bearing minerals. A major iron pool in terrestrial and aquatic systems are iron oxides (unless otherwise noted, in this review the term "iron oxides" is used as a general term for the various iron oxide, iron oxyhydroxide and amorphous iron hydroxide phases that are found in soil and aquatic systems). In soils, these minerals form as weathering products of primary minerals such as silicates and sulfides. In marine HNLC regions, iron oxides are supplied by atmospheric deposition.

The purpose of this review is to discuss the effect of siderophores on iron oxide solubility, dissolution mechanisms, and rates in the context of biological iron acquisition by terrestrial and marine organisms. For in depth discussion of various related issues the reader may consult a number of excellent review articles (Albrecht-Gary and Crumbliss, 1998; Boukhalfa and Crumbliss, 2002; Crumbliss, 1991; Hersman, 2000; Raymond et al., 1984; Roosenberg et al., 2000; Telford and Raymond, 1996; Wilhelm, 1995). A standard reference for iron oxide geochemistry is Cornell and Schwertmann, 2003. For a useful review on the surface chemistry of metal oxides, consult Brown Jr. et al., 1999.

This review focuses on biological iron acquisition in aerobic systems. Reducing conditions lead to a strong increase of iron solubility and it is unlikely to encounter iron limiting conditions in reducing systems. However, it is important to note that photo redox reactions can lead to increased steady state concentrations of Fe(II) in iron-limited aerobic systems such as marine surface waters.

Chemical structures of siderophores

Siderophores are organic ligands that are defined by their affinity and specificity for iron and their biological function in iron acquisition but not by their chemical structure. However, some commonalities in chemical structure exist amongst the almost 500 known siderophores (Boukhalfa and Crumbliss, 2002). Molecular masses of siderophores typically range from 0.5–1.5 kDa (Matzanke et al., 1989). Metal binding groups among microbial siderophores include α-hydroxycarboxylate, hydroxamate, catecholate, and less frequently carboxylate groups. The mugineic acid type plant siderophores have carboxylate, hydroxyl, and amine binding groups (Fig. 1). Most but not all siderophores are hexadentate ligands completely satisfying the inner coordination sphere of iron in 1:1 complexes. Bisucaberin (Fig. 1) is an example of a macrocyclic tetradentate siderophore forming 2:3 ferric complexes (Fe_2L_3) at and above neutral pH. Macrocyclic siderophores often exhibit higher affinity for Fe(III) in solution compared to their linear analogs in part due to preorganization effects (Hou et al., 1998; Spasojeviæ et al., 1999). For a list of formation constants

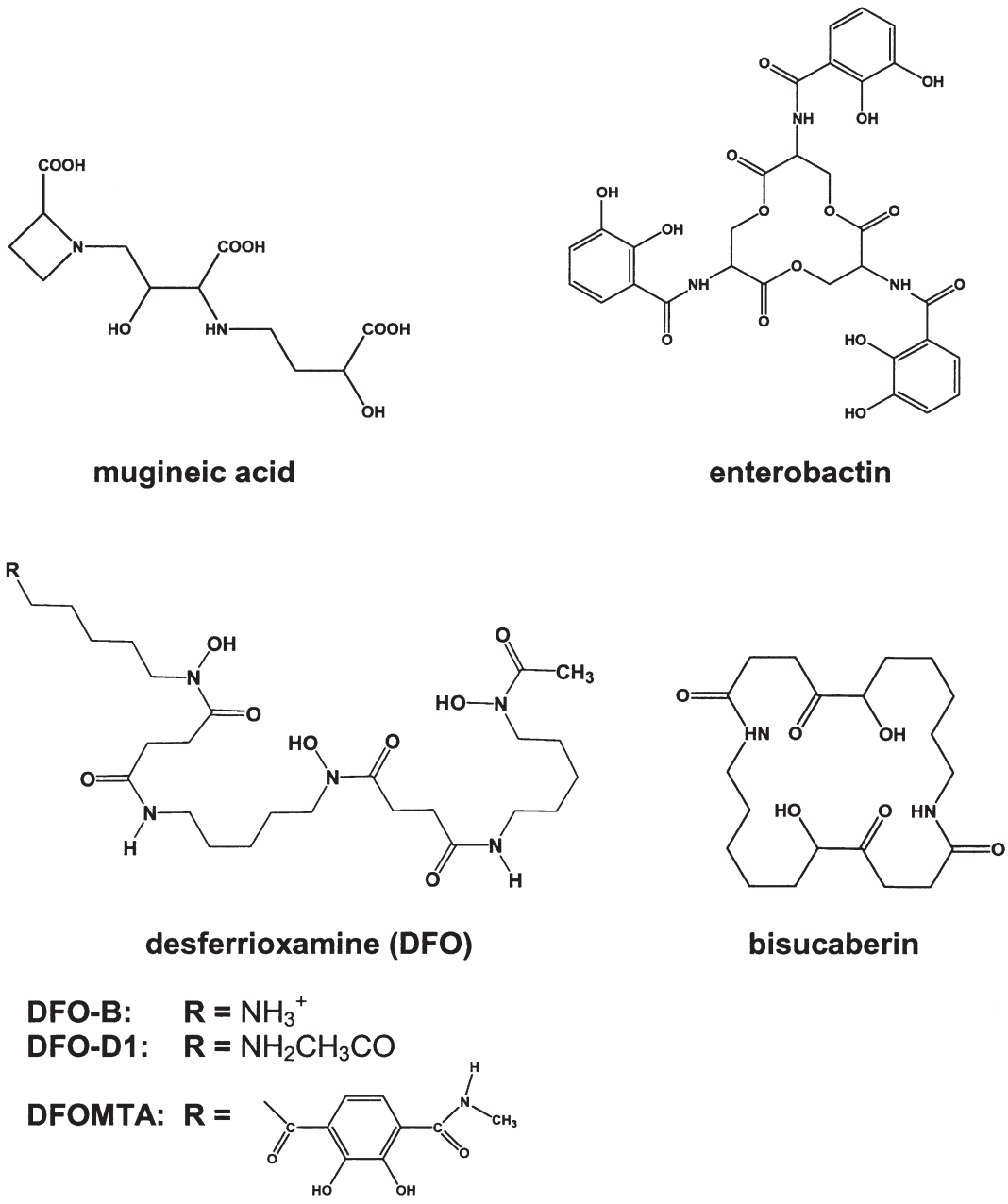

Figure 1. Molecular structures of plant and bacterial siderophores and of a synthetic derivative of a bacterial siderophore. Mugineic acid is a derivative of the structurally related phytosiderophores produced by graminaceous plants such as barley and wheat. Enterobactin is a catecholate siderophore produced by bacteria including *Escherichia coli*. Desferrioxamines are trihydroxamate siderophores produced by bacteria including the soil bacterium Streptomyces pilosum. DFOMTA is a synthetic derivative of DFO-B with specificity for binding of tetravalent actinides (Telford and Raymond, 1996). Bisucaberin is an example of a tetradentate macrocyclic dihydroxamate siderophore, isolated from the marine bacterium *Alteromonas haloplanktis*.

used for example calculations in this review, please see Table 4.

Hydroxamate functional groups form solution complexes with Fe(III) by loss of a proton from the hydroxylamine (–NOH) group and bidentate bonding with the carbonyl and hydroxylamine groups, resulting in a five membered ring (Crumbliss, 1990). Catecholate groups of siderophores such as enterobactin (Fig. 1) also form five membered rings with iron via the phenolic oxygens after loss of two protons in the neutral and alkaline pH range. At low pH, enterobactin coordinates iron in a "salicylate mode" via one phenolic oxygen and an ortho carbonyl group (Raymond et al., 1984).

Iron can also be mobilized by exudation of non-siderophore ligands. For example, cluster roots of plant species such as *Lupinus albus* exude citrate with high

exudation rates and acidify the rhizosphere even in calcareous soils (Dinkelacker et al., 1989). Also, root responses to iron stress are not limited to siderophore exudation. A comprehensive quantification of barley root exudates under iron stress revealed that in addition to siderophores up to 50% (expressed as µmole/g root tissue) of exuded organic ligands were other organic acids such as lactate, succinate, fumarate, malate, acetate, and amino acids (Fan et al., 1997). Some of these ligands are known to promote the dissolution of iron oxides. Low molecular weight organic ligands are ubiquitous in soil and aquatic systems and may also influence microbial iron acquisition. A discussion of the effect of siderophores on dissolution rates must therefore include a study of synergistic or inhibitory effects of low molecular weight organic ligands.

Siderophore concentrations in natural systems

Siderophore concentrations in most natural systems are low. Studies of marine systems have reported concentrations of strong iron complexing ligands between 0.3 and 7 nM (Gledhill and van den Berg, 1994; Gledhill et al., 1998; Powell and Donat, 2001; Rue and Bruland, 1997; van den Berg, 1995; Witter and Luther 1998; Wu and Luther, 1995). In soil solutions siderophore concentrations depend strongly on the soil horizons and higher concentrations occur in the rhizosphere compared to bulk soil (Bossier et al.,1988 and references; Nelson et al., 1988). Also, field experiments with *Pseudomonas fluorescens* containing an iron-regulated promoter fused to an ice nucleation reporter gene showed that the production of siderophores is a function of soil pH in the rhizosphere as predicted from laboratory experiments (Loper and Henkels, 1997). Powell et al. (1980) have estimated hydroxamate siderophore concentrations in soil solutions between 10^{-7} and 10^{-8} M.

Voelker and Wolf-Gladrow (1999) have calculated that the exudation of siderophores by marine cyanobacteria at low population densities is a costly strategy in terms of cellular nutrient and energy budgets. They concluded that the efficiency of siderophore production increases with increasing cell density. This is consistent with observations of increasing siderophore concentrations in the order marine environment < bulk soil < rhizosphere. Even higher siderophore concentrations may be reached in microenvironments such as biofilms, unless pH depression and/or anaerobic conditions in the microenvironment increase the solubility of iron, depressing siderophore production (Liermann et al., 2000).

Plants are able to exude phytosiderophore at high rates into the rhizosphere. Roemheld (1991) has estimated that phytosiderophore concentrations in the rhizosphere can reach local concentrations of up to 1 mM in the soil solution.

The solubility of iron oxides

As discussed above, in most environments, iron deficiency is not triggered by low total iron concentrations but by low solubility and dissolution kinetics of iron-bearing mineral phases. The solubility of iron oxides in aerobic systems depends on properties of the solid and the composition of the solution. Solubilities increase with decreasing particle sizes and increasing bulk lattice energies of iron oxides. Size and lattice energy are influenced by ageing and isomorphous substitution by metal ions such as Al(III). The solution pH, ionic strength, and the presence of organic ligands are key factors influencing the solubility of iron oxides.

The most common Fe(III) oxides in soils are hematite and goethite. Ferrihydrite may control the soluble iron concentrations in soil solutions due to its high solubility, surface area, and kinetic lability even if it represents only a minor iron pool. However, with decreasing crystal sizes the solubilities of goethite and hematite increase and can approach the solubility of ferrihydrite (Table 1; Langmuir, 1969; Trolard and Tardy, 1987). Particle diameters of soil goethite and hematites are in the nanometer range (10–150 nm, Cornell and Schwertmann, 2003). Partial isomorphous substitution of Fe(III) by Al(III) in the crystal structures of goethite and hematite is commonly found in soil minerals. It has been predicted that substitution by Al(III) decreases the standard free energy of the iron oxides and lowers their solubility, but no measured solubil-

Table 1. Solubilities of selected iron oxides.

Oxide	Log K_s [a]	pH_{PPZC}	$[Fe]_{tot}$ at pH = 8.0 [M]
hematite α-Fe_2O_3	−0.53 [b]	8.5 [g]	1.7×10^{-13}
goethite α-FeOOH	0.36 [b]	9.0–9.7 [g]	1.3×10^{-12}
goethite crystal size 100 nm [d]	0.63 [c]	–	2.5×10^{-12}
goethite crystal size 10 nm [d]	3.09 [c]	–	7.1×10^{-10}
goethite crystal size 8 nm [d]	3.77 [c]	–	3.4×10^{-9}
ferrihydrite	3.55 [e]	7.8 [h]	2.0×10^{-9}
"soil Fe-oxide"	2.70 [f]	–	2.9×10^{-10}

[a] $K_s = \{Fe^{3+}\}/\{H^+\}^3$ at infinite dilution and 298.15 K.
[b] Parker and Khodakovskii, 1995.
[c] calculated according to Langmuir, 1969 using bulk log $K_s = 0.36$.
[d] cube edge length [nm].
[e] Schindler et al., 1963.
[f] Lindsay, 1979.
[g] Sverjensky, 1994.
[h] measured pzc (Charlet and Manceau, 1992).

ity products of substituted iron oxides are available (Cornell and Schwertmann, 2003).

The solubility of iron oxides is also strongly influenced by the solution pH. Minimum solubilities are observed in the neutral to alkaline pH-range (see Fig. 2). This corresponds to the pH of soil solution in carbonatic soils (pH 7.5–8.5; Scheffer and Schachtschabel, 2002) and ocean water (circa pH 8.1; Wilson, 1975). The solubility of iron in equilibrium with "soil iron oxide" (aged ferrihydrite; Cornell and Schwertmann, 2003) in the absence of complexing ligands is below 2 nM at pH > 7 (Lindsay, 1979). Kuma et al., 1998 measured solubilities of ferrihydrite in the North Pacific Ocean between 0.14 and 3.6 nM (pH 8.0 – 8.2).

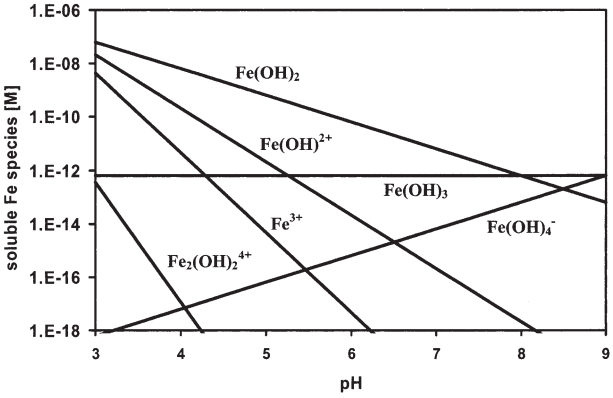

Figure 2. Calculated solubility of iron in equilibrium with goethite and iron speciation as a function of pH. For solubility product constants and equilibrium constants for iron hydroxo species, see Table 4.

Effects of siderophores on iron oxide solubility

Increasing the iron oxide solubility by formation of soluble iron complexes is an important function of siderophores in biological iron acquisition. This can be expressed by combining the dissolution reaction (e.g., of goethite) and the corresponding solubility product K_S with the complexation reaction of iron (e.g., by a trihydroxamate siderophore) and the corresponding stability constant K_{FeL}:

$$\alpha - FeOOH + 3H^+ \leftrightarrow Fe^{3+} + 2H_2O \qquad K_S \qquad (1)$$

$$Fe^{3+} + H_3L \leftrightarrow FeL + 3H^+ \qquad K_{FeL} \qquad (2)$$

and writing a dissolution reaction in the presence of a siderophore:

$$\alpha - FeOOH + H_3L \leftrightarrow FeL + 2H_2O \qquad K_{S,L} \qquad (3)$$

with the corresponding mass law:

$$K_{S,L} = \frac{FeL}{H_3L} \quad \text{or}$$

$$FeL = H_3L \times K_{S,L} = H_3L \times K_S \times K_{FeL} \qquad (4)$$

Where $K_{S,L}$ is the product of the solubility constant of the iron oxide and the stability constant of the iron-siderophore complex (for simplicity, coupled deprotonation and hydrolysis reactions are not included here). The concentration of the dissolved iron complex at constant pH increases with the free ligand concentration, the solubility product of the iron oxide, and the stability constant of the Fe-siderophore complex.

Given the low solubility of iron oxides at neutral and alkaline pH and the low concentrations of ligands in terrestrial and marine systems, the high affinity of the siderophores for iron binding is a prerequisite for increasing iron oxide solubility. As shown in Figure 3, decreasing affinities of ligands for iron in the order DFO-B > MA > oxalate leads to decreasing soluble iron concentrations at equal total ligand concentrations. The lower affinities of phytosiderophores compared to microbial siderophores is partly compensated for by high exudation rates by graminaceous plant roots resulting in local ligand concentrations in the millimolar range in the rhizosphere (Roemheld, 1991). Assuming that microbial siderophore concentrations in the soil are typically in the sub-micromolar range (Powell et al., 1980) phytosiderophores can have an equal or higher effect on the iron oxide solubility compared to microbial siderophores at typical soil concentrations. Oxalate has little effect on goethite solubility at pH 8 in concentrations below one mM.

Figure 4 illustrates the effect of pH on the solubility of goethite in the presence of DFO-B, mugineic acid and oxalate compared to the solubility in the absence of organic ligands. 1 mM Oxalate has a high affinity for iron at low pH, but above neutral pH its effect on goethite

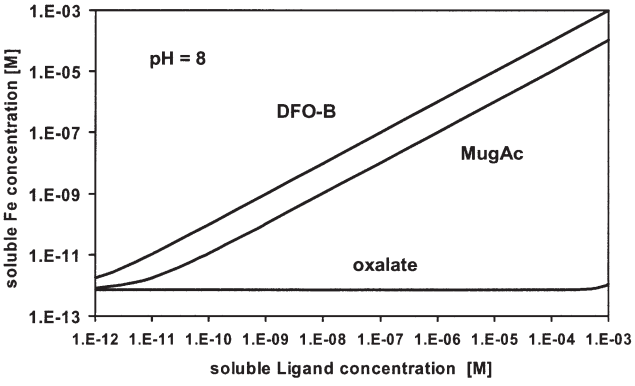

Figure 3. Calculated soluble iron concentrations in equilibrium with goethite at pH 8 as a function of soluble ligand concentrations. Ligands are DFO-B, mugineic acid, or oxalate respectively.

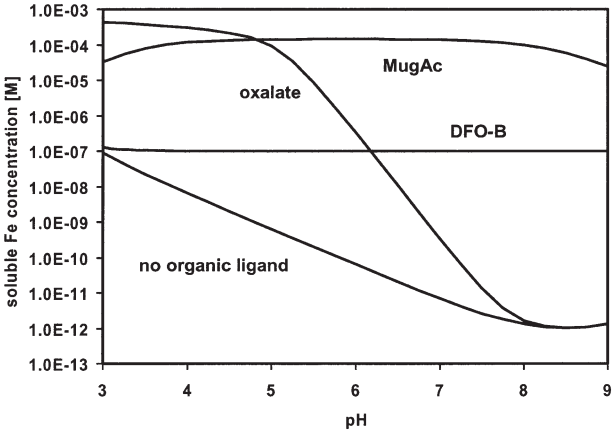

Figure 4. Calculated soluble iron concentrations in equilibrium with goethite as a function of pH in the presence of 10^{-7} M DFO-B, 10^{-3} M mugineic acid, 10^{-3} M oxalate, or no organic ligand respectively.

solubility rapidly degrades. In contrast, the presence of 1mM mugineic acid and 0.1 µM DFO-B (concentrations chosen to reflect soil siderophore concentrations) increase goethite solubility over a wide pH range.

Rate laws of iron oxide dissolution

From a thermodynamic standpoint, the affinity of siderophores for iron and the concentrations at which they occur in the environment should be sufficient to increase soluble iron concentrations to adequate levels to support microbial and plant growth. However, as Römheld (1991) pointed out: "Insufficient consideration of kinetic aspects is another reason why conclusions which are based on equilibrium chemistry are inadequate. Besides solubility at equilibrium, the dissolution rates (kinetic aspects) of Fe oxides in soils determine the supply of Fe to the plant root." The kinetic aspects of iron oxide dissolution in the presence and absence of siderophores are discussed in this section.

Fe(III) ions in iron oxides are usually octahedrally coordinated by oxygen, hydroxyl anions, and water. In the bulk of the mineral grains all coordinative partners of iron are part of the crystal lattice. At the mineral surface, Fe(III) is partially coordinated by the crystal lattice, and partially by adsorbed water or OH^-. The dissolution process can be interpreted as a progressive exchange of the crystal lattice as coordinative partner by adsorbed ligands. The overall dissolution rates are determined by the rate of this progressive ligand exchange reaction. Processes that increase the kinetic lability of the coordinative bonds between surface iron ions and the lattice accelerate the dissolution reaction. These processes are:

– reduction of Fe(III) to Fe(II) → reductive dissolution
– protonation of lattice O or OH groups in the inner coordination sphere of surface Fe(III) ions → proton-promoted dissolution
– coordination of surface Fe(III) by organic or inorganic ligands, leading to a kinetic labilization of other bonds in the inner coordination sphere → ligand-controlled dissolution

Under the assumption that parallel dissolution mechanisms are independent, the rate law of non-reductive dissolution is:

$$R_{net} = (R_H + R_{OH} + \Sigma R_{Ln})\, f(\Delta G) \qquad (5)$$

where R_H and R_{OH} [mole m^{-2} h^{-1}]are the rates of proton-promoted and alkaline dissolution respectively, R_{L1}, R_{L2}… R_{Ln} are the rates of ligand-promoted dissolution in the presence of ligands L_1 to L_n, including siderophore ligands, and $f(\Delta G)$ is a function of the solution saturation sate with respect to the dissolving mineral (Furrer and Stumm, 1986; Kraemer and Hering, 1996).

Proton-promoted dissolution

Proton-promoted dissolution involves the protonation of coordinative partners of iron ions at the mineral surface. Proton-promoted dissolution rates of goethite are related to surface excess of adsorbed protons (in excess of the protonation state at the ZPC):

$$R_H = k_h [H_{ads}]^n$$

where k_h is the rate constant of proton-promoted dissolution and n is the reaction order (3.25 for goethite according to Zinder et al., 1986). This is consistent with a mechanism involving the protonation of three O/OH groups in the inner coordination sphere of surface iron (Wieland et al., 1988). The triply protonated surface site is the precursor to the rate determining step in the overall dissolution reaction. After the detachment of the iron ion, the surface structure is restored by further surface protonation. The protonation state of the mineral surface is related to the pH in a non-linear way, leading to fractional reaction orders if the rate law is expressed in terms of pH. Alkaline dissolution can be seen as a special case of ligand-controlled dissolution with the deprotonation of adsorbed water or hydroxyl leading to an increase of their labilizing effect.

In the context of biological iron acquisition it is important to note that the combined proton-promoted and alkaline dissolution rates have a minimum in the same pH range in which iron oxides have a minimum solubility, i.e., in the neutral to alkaline pH range. This means that in the absence of complexing ligands, iron acquisition in carbonatic soils and marine systems is not only limited by the low solubility of iron oxides, but also by their slow dissolution kinetics.

Ligand-controlled dissolution

Natural and anthropogenic ligands have an important influence on the weathering kinetics of oxide minerals (Casey and Ludwig, 1996; Furrer and Stumm, 1986; Kraemer and Hering, 1997). A generalized mechanism of ligand-controlled dissolution has been proposed (Furrer and Stumm, 1986) which includes three steps 1) fast surface complex formation by a ligand exchange mechanism, 2) slow, rate determining detachment of the surface metal center, 3) fast regeneration of the surface. It is assumed that the adsorbed ligand influences the dissolution rate by destabilization of the coordinated iron ions at the oxide surface, which is brought about by inductive effects enhancing electron density on adjacent oxo bonds (Wehrli et al., 1990). This effect is analogous to the acceleration of the exchange rates of metal coordinating water in the presence of coordinating organic ligands (trans effect) (Ludwig et al., 1995): the coordinating ligand destabilizes bonds in the metal ion coordination sphere and facilitates the bond breaking that is involved in either water exchange or dissolution. The rate constant of ligand-controlled dissolution k_L is influenced by changes in surface speciation of the ligand. The surface speciation can potentially be influenced by factors such as pH, surface coverage and the adsorption of other inorganic ligands (Kraemer and Hering, 1998).

The rate of ligand-controlled dissolution R_L is a function of the surface excess of adsorbed ligands and the nature of the $\equiv Fe-L$ surface complexes (Furrer and Stumm, 1986):

$$R_L = k'_L[\equiv Fe-L] \quad (6)$$

where k'_L is a pseudo first order rate constant [h^{-1}] and $[\equiv Fe-L]$ is the surface concentration of surface complexes that are precursors of the rate determining step [mole m^{-2}]. If the surface speciation remains constant over the experimental conditions, the rate law can be simplified to:

$$R_L = k_L[L]_{ads} \quad (7)$$

where $[L]_{ads}$ is the surface excess of adsorbed ligands [mole m^{-2}]. The formation of the precursor complex by adsorption of the ligand polarizes bonds between the iron ion and oxygen of the crystal lattice, thereby promoting the dissolution reaction. Any factor that influences the ligand surface concentration or speciation is also likely to influence dissolution rates. It is therefore important to consider the surface chemistry of siderophore on iron oxides in detail.

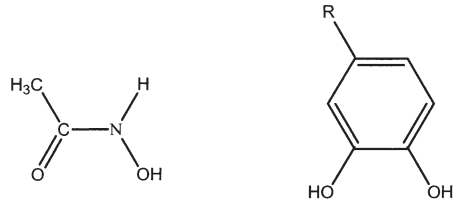

	acetohydroxamic acid (aHA)	R = H catechol	R = NO_2 4-nitrocatechol
pK_{a1}	9.29	9.26	6.69
pK_{a2}	-	13.3	10.83

Figure 5. Monohydroxamate and monocatecholate model compounds.

Adsorption of siderophores at the iron oxide surface

Among the surface chemical properties that make organic ligands effective for promoting iron oxide dissolution in marine systems and carbonatic soils, two derive directly from the rate law of ligand-controlled dissolution (Eq. 6):

1. the tendency to form inner sphere surface complexes
2. a high affinity for adsorption in the neutral to alkaline pH-range.

The lability of the inner coordination sphere of dissolved metal ions increases with increasing denticity of the coordinating ligands (Margerum et al., 1978). In analogy to this, bidentate surface complexes have a significantly greater effect on oxide dissolution kinetics than monodentate surface complexes (Furrer and Stumm, 1986; Ludwig et al., 1995). However, the number of bonds between an organic ligand and a single Fe(III) ion at the mineral surface is limited by the exchangeable partners in the inner coordination sphere. Among bidentate surface complexes, five membered rings have a higher effect on dissolution rates than 6 or 7 membered rings. The simultaneous coordination of adjacent surface sites by a single ligand leads to inhibition of oxide dissolution (Bondietti et al., 1993). This discussion emphasizes a third condition for a high efficiency of a ligand for accelerating iron oxide dissolution:

3. the tendency to form mononuclear multidentate surface species.

Adsorption of organic ligands to iron oxide surfaces can be described by a ligand exchange reaction. Structural iron ions at the oxide water interface are partly coordinated by oxygen or hydroxyl ions of the crystal lattice and partly by adsorbed water or hydroxyl anions. Adsorption of ligands and formation of inner sphere surface complexes involves replacement of surface hydroxyl groups or water by a ligand exchange reaction (Kummert and Stumm, 1980; see also Fig. 6).

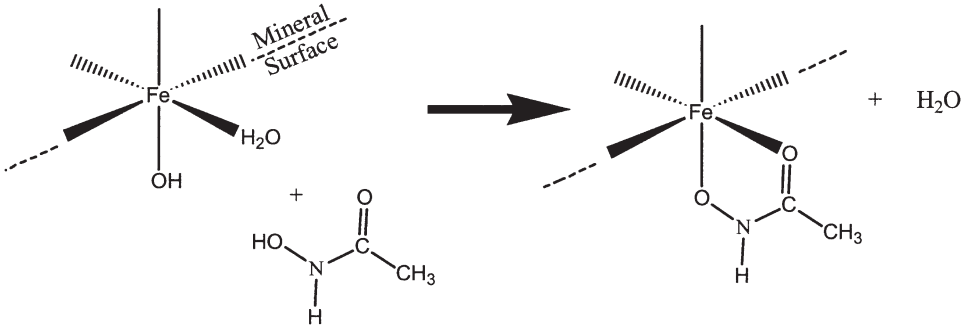

Figure 6. Adsorption of acetohydroxamic acid by a ligand exchange reaction (after Holmen and Casey, 1996).

The overall standard free energy change of the adsorption reaction includes contributions from the standard free energy change of the ligand exchange reaction (ΔG^0_{chem}), of electrostatic interactions with the mineral surface ($\Delta G^0_{coulomb}$), and of hydrophobic interactions ($\Delta G^0_{hydroph}$):

$$(\Delta G^0 = \Delta G^0_{chem} + G^0_{coulomb} + \Delta G^0_{hydroph}$$

The coordination properties of Fe(III) and the incoming ligands have an important effect on ΔG^0_{chem}. Fe(III) is a hard cation with a high charge to radius ratio. It therefore favors coordination by ligands with hard O donor atoms such as the catecholate, hydroxamate, or α-hydroxycarboxylate groups of siderophores. The resulting bonds have a highly ionic character. In analogy to its coordination chemistry in solution, preferential surface complexation of Fe(III) on iron oxide surfaces by hard ligands is evidenced by high affinities of ligands with o-donor atoms for adsorption. Examples of bidentate hard ligands with both a high affinity for Fe(III) in solution and at the mineral surface are the catecholate and hydroxamate functional groups of siderophores, citric acid, ascorbic acid, salicylic acid, and oxalic acid.

Electrostatic interactions are important for inner sphere adsorption if the surface complex formation changes the overall charge of a surface site. Hydrophobic interactions become important if the surface excess of adsorbed hydrophobic substances is high enough to allow for interactions among hydrophobic moieties of the adsorbed substances. A classic example is the formation of hemi micelles at high adsorbed surfactant concentrations (Fuerstenau and Colic, 1999).

Adsorption of monohydroxamate and monocatecholate ligands

To gain a better understanding of the surface chemistry of siderophores, it is useful to consider detailed investigations of the adsorption and surface speciation of simple monohydroxamate and monocatecholate ligands.

Holmen et al. (1997) have elucidated the structure of the acetohydroxamic acid (aHA) surface complex on goethite by FTIR-spectroscopy. aHA adsorbs on the goethite-water interface by a ligand exchange reaction as shown in Figure 6. The aHA surface complex is a bidentate mononuclear five membered ring in analogy to the dissolved 1:1 Fe(III)-aHA complex. Casey and Holmen (1996) have found no net protonation or deprotonation of surface sites resulting from the adsorption of aHA. They concluded that there is no significant electrostatic contribution to the free energy change of the adsorption reaction. This contributes to an essentially constant adsorption envelope between pH 4 and 9.

The adsorption of 4-nitrocatechol and 4-nitro-1,2-phenylenediamine was investigated by Vaseduvan and Stone, 1998. The hydroxyl groups of 4-nitrocatechol are replaced by two amine groups in 4-nitro-1,2-phenylenediamine. Amine groups are soft ligands with a higher covalent and less ionic contribution to bonding. The hard ligand 4-nitrocatechol had a substantially higher affinity for adsorption on goethite and hematite surfaces then the soft ligand 4-nitro-1,2-phenylenediamine. Adsorption envelopes of 4-nitrocatechol on goethite and hematite and of catechol on hematite have broad adsorption maxima in the neutral and alkaline pH-range respectively (Gu et al., 1995; Vaseduvan and Stone, 1998).

This discussion indicates that monocatecholates and monohydroxamates fulfill the criteria for effective labilization of iron at the mineral surface as stated above: they form inner sphere surface complexes with a high affinity for adsorption on iron oxides in a pH range characteristic for carbonatic soils and the marine system. Also, mono hydroxamates are known to form mononuclear, bidentate surface complexes.

Adsorption of siderophores

In order to compare adsorption of monohydroxamate or monocatecholate ligands with siderophores, it is important to consider effects arising from the architecture, denticity and charge of the biogenic ligands. The conformation and

bonding of adsorbed multidentate siderophores are influenced by steric constraints imposed by the surface and the siderophore architecture, charge, and hydrophobicity.

Based on the surface density of Fe(III) ions with two "non-lattice" coordinative partners (i.e., adsorbed H_2O and OH^-) available for ligand exchange by a single hydroxamate group of a siderophore, and on the spacing of hydroxamate groups in DFO-B, Holmen and Casey, 1996, have argued that only mononuclear and binuclear surface complexes can form. They considered it unlikely that two hydroxamate groups can coordinate a single Fe(III) surface site in a stable surface complex. Cocozza et al., 2002, have argued that hydroxamate groups of DFO-B coordinate Fe(III) at iron oxide surfaces analogously to the aHA surface complex and that only a single hydroxamate group of adsorbed DFO-B is participating in surface complexation, coordinating surface sites analogous to adsorbed aHA. Their argument is supported by the observation of similarities of the compensation law (relating the pre-exponential factor to the apparent activation energy in the Arrhenius equations) for the complexation of Fe(III) by DFO-B and aHA in solution and at the mineral surface, and by similarities of the rate constants of ligand-controlled dissolution of goethite in the presence of DFO-B and aHA (see Table 2).

The effect of surface charge on siderophore sorption is illustrated in Figure 7 (Kraemer et al., 1999). DFO-B is a cationic species at pH < 8 due to protonation of the terminal amine group (pK_{a1} = 8.38). DFO-D_1 is an acetyl derivative of DFO-B which has no charge below pH 8.9. Electrostatic repulsion between the ligand and the positively charged oxide surface is resulting in lower adsorption of DFO-B compared to DFO-D_1 at pH < 8.

Non-specific interactions can arise from the hydrophobic backbone of DFO-B and DFO-D_1. Hydrophobic interactions result in adsorption of ligands in excess

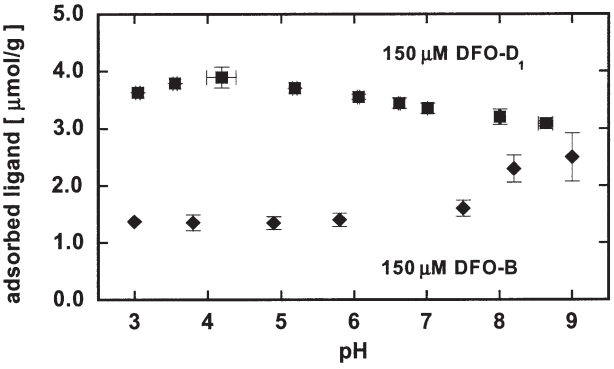

Figure 7. Adsorption envelope for DFO-B (diamonds) and DFO-D (squares) on goethite. Error bars indicate twice the standard deviation of duplicate sample measurements. The total ligand concentration was 150 µM; 0.01 M NaClO4; solid conc. 13 g/L, [MOPS] = 5 mM. Reprinted from Kraemer et al. (1999) Geochim. Cosmochim. Acta 63, 3003–3008, with permission from Elsevier.

of the surface concentration of Fe(III) surface sites at high total ligand concentrations (Evanko and Dzombak, 1999). This has not been observed in the case of DFO-B or DFO-D_1. On the contrary, very low maximum surface concentrations were measured for both siderophores, potentially indicating steric hindrance to adsorption. Such "umbrella effects", which effectively lower the maximum available surface sites for large ligands, have been observed for other ligands in similar molecular weight ranges (Kovacevic et al., 1998; Simpson et al., 2000). Neubauer et al., 2002, measured higher surface concentrations on goethite and on ferrihydrite after a reaction time of 8 and 7 days respectively. However, during that time significant iron dissolution occurred, potentially influencing adsorption behavior.

Cervini-Silva and Sposito (in preparation, a) observed that the ionic strength and the nature of anions in suspension affect the adsorption of siderophores on goethite and

Table 2. Rate constants, ligand surface excess, and rates of ligand-promoted dissolution of goethite in the presence of various siderophore and non-siderophore ligands in the pH range 5 to 6.5.

Ligand	pH	$[L]_{diss}$ [µM]	$[L]_{ads}$ [mole × m^{-2}]	k_L [h^{-1}]	E_{act} [kJ/mole]	R_L [mole × m^{-2} × h^{-1}]	Reference
DFO-B	5	80	0.37×10^{-7}	0.015	28.5	0.57×10^{-9}	Kraemer et al., 1999 Cheah et al., 2003 Cocozza et al., 2002
DFO-D_1	6.5	240	1.6×10^{-7}	0.06	21.7	9.4×10^{-9}	Kraemer et al., 1999 Cocozza et al., 2002
aHA	6	100	2.2×10^{-7}	0.01	–	2.2×10^{-9} [a]	Holmen and Casey, 1996
Oxalate	5	100	10×10^{-7}	0.001	–	1×10^{-9} [a]	Cheah et al., 2003
EDTA	5.3	7	18×10^{-7}	0.0016	–	2×10^{-9}	Nowack and Sigg, 1997
Proton-promoted dissolution at pH = 5					98–100 [b]	0.28×10^{-9} [a]	Zinder et al., 1986 Cornell et al., 1976

[a] Calculated.
[b] E_{act} of proton-promoted dissolution.

its dissolution. Increasing the electrolyte concentration results in a positive change of surface excess of siderophores, and a decrease in the rate of Fe release. Irrespective of the counter anion coordinating properties (i.e., ClO_4^- or Cl^-), DFO-B adsorption on goethite as affected by the ionic strength followed a positive linear function. Congruency between goethite net surface charge and DFO-B surface excess in NaCl, but not $NaClO_4$, medium substantiated the role of chloride as promoter on DFO-B adsorption. Evidently, the presence of Cl^- affected the intrinsic affinity of siderophores for iron (hydr)oxides surface. The negative salt effect on dissolution kinetics data was explained because ion-pairing mechanism and the formation of Fe(DFO-B)(Cl) ternary surface complexes.

An FTIR investigation of parabactin (a tricatecholate siderophore) adsorbed on aluminum oxide films indicated surface complexation through the hydroxyl groups of catechol groups (Hansen et al, 1995). However, presently there is little spectroscopic evidence available that allows an unambiguous elucidation of siderophore surface complexes.

The kinetics of siderophore-controlled dissolution of goethite

The dissolution rates of goethite in the presence of DFO-B have been investigated by Kraemer et al., 1999; Cocozza et al., 2002, and Cheah et al., 2003. Cheah et al., 2003, have observed a linear relationship between the surface excess of siderophores and dissolution rates. They concluded that siderophore-controlled dissolution is surface-controlled and can be described by the rate law Equation 6.

The rate law of ligand-controlled dissolution (Eq. 6) states that the favorable thermodynamic stability and surface concentration of the surface complex combined with its kinetic lability are essential for the efficient acceleration of the dissolution reaction. Both factors need to be taken into account when comparing ligand-controlled dissolution kinetics in the presence of siderophores and other ligands (Table 2). Goethite dissolution rate constants in the presence of oxalate and EDTA are one order of magnitude lower compared to rate constants of DFO-B and DFO-D_1-promoted dissolution. However, similar dissolution rates are observed at equal or lower dissolved oxalate or EDTA concentrations compared to siderophore concentrations. This is illustrated by comparing calculated "far from equilibrium" goethite dissolution rates in the presence of oxalate and DFO-B as a function of the soluble ligand concentrations (Fig. 8). At equimolar dissolved concentrations, oxalate is more effective then DFO-B in promoting goethite dissolution. The reason for the efficiency of the non-siderophore ligands is the higher

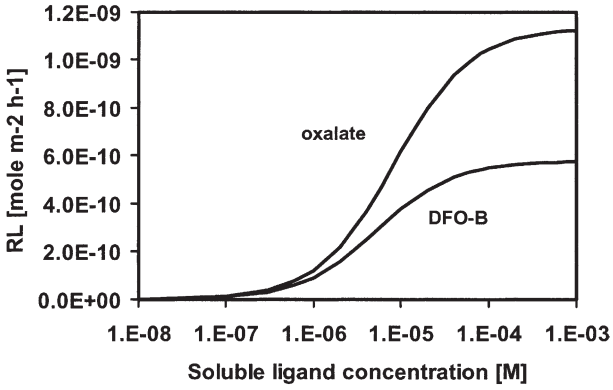

Figure 8. Calculated ligand-controlled dissolution rates of goethite as a function of soluble oxalate or DFO-B concentrations 'far from equilibrium' (i.e. assuming that the solution is strongly under saturated with respect to goethite). Rates were calculated using Equation 7. Ligand surface excesses were calculated using a Langmuir isotherm. Langmuir parameters and rate constants from Cheah et al., 2003. pH = 5.

surface excess of adsorbed oxalate and EDTA at similar soluble concentrations. Kraemer et al. (1999) have observed a maximum surface excess of DFO-B of 0.43×10^{-7} mole $\times$ m^{-2} compared to a maximum surface excess of oxalate and EDTA of 11×10^{-7} mole $\times$ m^{-2} and 19×10^{-7} mole $\times$ m^{-2} respectively (Cheah et al., 2003; Nowack and Sigg, 1996). As discussed above, the reason for the limited adsorption of DFO-B and DFO-D_1 on goethite is still uncertain. This illustrates the need of spectroscopic information on the surface speciation of siderophores in order to get a full understanding of siderophore-controlled iron oxide dissolution as part of biological iron acquisition strategies.

Cervini-Silva and Sposito (2002) have investigated the effect of isomorphous Al substitution (2.6–10 mol% Al) on goethite dissolution rates in the presence of DFO-B, oxalate, and in 6 M HCl respectively. They found that increasing level of Al substitution lead to decreasing proton-promoted dissolution rates, increasing siderophore-controlled dissolution rates, and had no effect on oxalate-controlled dissolution. Incongruent dissolution due to preferential release of Al was observed in proton- and oxalate-promoted dissolution. Dissolution in the presence of DFO-B was approximately congruent. An increase of goethite dissolution with increasing Al substitution has also been observed in the presence of siderophore producing bacteria (Maurice et al., 2000). Cervini-Silva and Sposito (submitted, b) compared the dissolution rates of goethite and hematite in the presence DFO-B, DFO-D1, and DFOMTA at neutral pH. DFOMTA[N-(2,3-dihydroxy-4-(methylamido)benzoyl)desferrioxamine B], is a derivative of DFO-B prepared by attaching a catecholate group to the free amine group (Fig. 1). The molecular structure of siderophores influences the rate of dissolution of iron (hydr)oxides at circumneutral pH. Dissolu-

tion kinetics data indicate that the order of reaction with respect to siderophore concentration becomes increasingly positive as the residual charge throughout the siderophore molecules becomes increasingly negative. A linear correlation found among the dissolution of hematite and goethite by DFOMTA, DFO-B, and DFO-D1 points to a common mechanism for Fe complexation as the controlling step during siderophore-promoted dissolution.

Hersman et al., 1995, observed hematite dissolution rates at pH 3 in the presence of 240 µM of a pseudobactin type siderophore. They found that the siderophore-controlled dissolution rates were lower than oxalate-promoted or ascorbate-promoted dissolution rates at ligand concentrations of 1 mM respectively. A study of goethite and ferrihydrite dissolution rates in the presence of the marine siderophore biscaberin (produced by *Alteromonas haloplanktis*) in artificial seawater was conducted by Yoshida et al., 2002. Interestingly, they found higher surface area based dissolution rates for goethite compared to ferrihydrite over the pH range 4–8 at equal siderophore concentrations. However, mass based dissolution rates were higher for ferrihydrite compared to goethite due to the higher surface area of ferrihydrite. For both ferrihydrite and goethite dissolution rates decreased with increasing pH.

Dissolution rates of hornblende and kaolinite by DFO-B have been measured by Kalinowski et al., 2001, and Rosenberg and Maurice, 2003. The observed rates vary by more then two orders of magnitude. The lower dissolution rates form kaolinite compared to hornblende was attributed to the low iron content of the clay mineral (Rosenberg and Maurice, 2003). DFO-B enhanced the release of Fe, Si, and Al from hornblende and kaolinite. Both groups have concluded that ligand-promoted dissolution is surface-controlled.

The ability of phytosiderophores to dissolve iron oxides has been verified previously (Hiradate and Inoue, 1998a, b; Inoue et al., 1993). It was found that mugineic acid (see Fig. 1) can solubilize iron within 4 hours reaction time from various iron oxides in the order ferrihydrite >> lepidocrocite ≥ goethite = hematite. However, information on dissolution rates and the mechanisms of phytosiderophore-controlled dissolution is not available.

A number of studies have dealt with the dissolution of iron-bearing minerals in bacterial and fungal cultures or in the rhizosphere of plants. Examples include the dissolution of hematite, goethite, Al-substituted goethite, ferrihydrite, and kaolinite in cultures of *Pseudomonas mendocina* (Hersman et al., 1996, 2001; Maurice et al., 2000, 2001a, 2001b), the dissolution of hornblende by *Streptomyces sp.* and *Arthrobacter sp.* (Kalinowski et al., 2000; Liermann et al., 2000), the dissolution of goethite by the fungus *Suillus granulatus* (Watteau and Berthelin, 1994), and the dissolution of iron sulfides, -phosphates, -oxides, and iron-bearing silicates in the presence of *Azotobacter vinlandii* (Page and Huyer, 1984). The interpretation of these finding in terms of mineral surface chemical mechanisms is difficult. A number of kinetically controlled processes influence iron and siderophore concentrations in solution such as siderophore exudation, uptake, and degradation, iron oxide dissolution, iron uptake and recycling, microbial growth rates and so on. Several researchers have therefore based their interpretation of bacterial iron acquisition on microbial growth rates and population sizes in the presence and absence of iron-bearing minerals (Hersman et al., 1996, 2001; Maurice et al., 2000, 2001a, 2001b). It is difficult to asses the effect of bacterial growth media on mineral surface chemistry. For example, high concentrations of phosphate in the nutrient solution potentially inhibit siderophore-controlled dissolution (Bondietti et al., 1993). For a review of experimental approaches, see Kalinowski et al., 2000 and Hersman, 2000. Experiments involving bacterial cultures in the presence of relevant iron pools are a necessary step towards a full understanding of siderophore-controlled iron acquisition in natural systems.

Table 3. Siderophore-promoted dissolution rates of iron oxides and iron-bearing silicates in the presence of various siderophores.

Mineral	Siderophore	$[L]_{total}$ [µM]	pH	R_L [mole × m^{-2} × h^{-1}]	Reference
Hematite	Pseudobactin type	240	3	10×10^{-9}	Hersman et al., 1995
Ferrihydrite	Biscaberine	0–12.9 [a]	3.9–8.2	$0.4 - 3.4 \times 10^{-9}$ [b]	Yoshida et al., 2002
Goethite	Biscaberine	0–12.9 [a]	3.9–8.2	$1.4 - 9.5 \times 10^{-9}$ [b]	Yoshida et al., 2002
Hornblende	DFO-B	24–240	7.2–7.5	$14 - 40 \times 10^{-9}$	Lierman et al., 2000
Kaolinite	DFO-B	240	3–7	$\sim 0.1 \times 10^{-9}$	Rosenberg and Maurice, 2003
Al-substituted goethite	DFO-B	20–1000	5	$0.07 - 30.5 \times 10^{-9}$	Cervini-Silva and Sposito, 2002

[a] Expressed as iron complexing capacity as measured by CAS-assay.
[b] In artificial seawater.

The effect of siderophores on the solution saturation state of iron oxides

A rate law describing the influence of the solution saturation state on dissolution rates has been derived from the activated complex theory and the law of detailed balancing (Aagaard and Helgeson, 1982; Lasaga, 1981). This empirical rate law has been applied to ligand-controlled dissolution of iron oxides (Kraemer and Hering, 1997):

$$R_{net} = \Sigma k_{Ln}[L_n]_{ads}\left[1 - \exp\left(\frac{\Delta G}{\sigma \mathrm{RT}}\right)\right] \quad (8)$$

where $\Sigma k_{Ln}[L_n]_{ads}$ are the rates of ligand-controlled dissolution in the presence of the ligands L_1 to L_n; ΔG is the Gibbs free energy of reaction [kJ mole^{-1}]; R is the gas constant and T is the absolute temperature [K]. σ has been experimentally determined with $\sigma = 2$ for ligand-controlled dissolution of goethite (for a discussion of the physical meaning of σ, see Boudart and Djega-Mariadassou, 1984; Temkin, 1971).

The term $f(\Delta G) = [1 - \exp(\Delta G/2\mathrm{RT})]$ describes the effect of the solution saturation state (expressed as Gibbs free energy of the dissolution reaction) on dissolution rates. It reaches a constant value of unity far from equilibrium (i.e. strong undersaturation / $\Delta G << 0$). As equilibrium is approached ($\Delta G = 0$), $f(\Delta G)$ goes to zero (Fig. 9). The solution saturation state has little effect on net dissolution rates at $\Delta G < -8$ kJ/mole since $f(\Delta G) > 0.9$ and the net rate of dissolution approximates the maximum dissolution rates so that equation 8 simplifies to Equation (7) ($R_{net} \sim \Sigma k_{Ln}[L_n]_{ads}$). More then 50% of maximum dissolution rates are expected at $\Delta G < -3$ kJ/mole.

The effect of siderophores on ΔG can be illustrated by an example where the solution saturation state with respect to goethite at pH = 8 and in the presence of dissolved concentrations of 10^{-7} M DFO-B or 10^{-3} M oxalate is shown as a function of total dissolved iron concentrations (Fig. 10). Oxalate has little effect on the solubility of goethite at pH 8 (compare with Figs. 3 and 4). Therefore, the solution is over-saturated with respect to goethite at iron concentrations above 10^{-12} M and in the presence of 1 mM oxalate. Due to its high affinity for Fe(III), 10^{-7} M DFO-B essentially solubilizes equimolar concentrations of Fe(III) in equilibrium with goethite (i.e., $\Delta G = 0$) at pH 8.

An important result of this model calculation is that an excess of 10 nM dissolved DFO-B over the dissolved iron concentration is sufficient to decrease ΔG to below -8 kJ/mole, minimizing the effect of the solution saturation state on dissolution rates. An excess of only 0.1 nM DFO-B is needed to decrease ΔG to below -3 kJ/mole. In other words, only minute excess concentrations in the order of several nM of the siderophore in solution are needed to provide sufficient Gibbs free energy to drive any ligand-controlled dissolution mechanism, including those involving non-siderophore ligands. Such a disequilibrium can be attained if siderophore exudation rates exceed the iron oxide dissolution rates.

Experimental evidence of this function of siderophores is provided by Cheah et al., 2003, where it was shown that the presence of siderophores in the micro molar concentration range reduced the Gibbs free energy sufficiently to accelerate an oxalate-controlled dissolution mechanism at pH 5. This is of great importance as oxalate and other low molecular weight organic ligands are ubiquitous in soil systems. However, in the alkaline pH-range, adsorption of non-siderophore ligands usually decreases with increasing pH. For example, oxalate will have little effect on dissolution rates at pH 8 due to its low affinity for adsorption at this pH. However, humic and fulvic substances as well as biogenic exudates have functional groups which can impart significant affinity for sorption above pH 8 (e.g. citrate (Filius et al., 1997)).

Conceptually the effect of siderophore ligands on iron oxide dissolution is twofold: 1) adsorbed siderophores

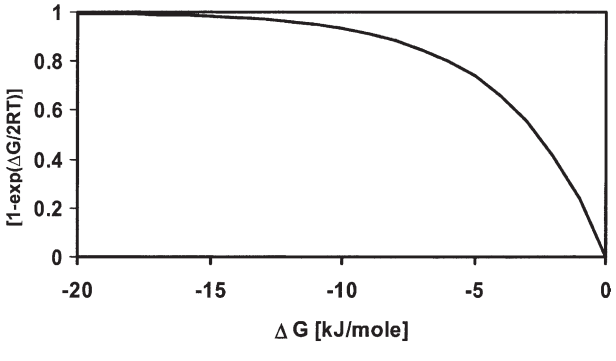

Figure 9. Effect of solution saturation state (expressed as Gibbs free energy change of reaction) on dissolution rates using Equation 8. At low ΔG, dissolution rates are approaching constant maximum rates. At $\Delta G = 0$, dissolution rates are zero.

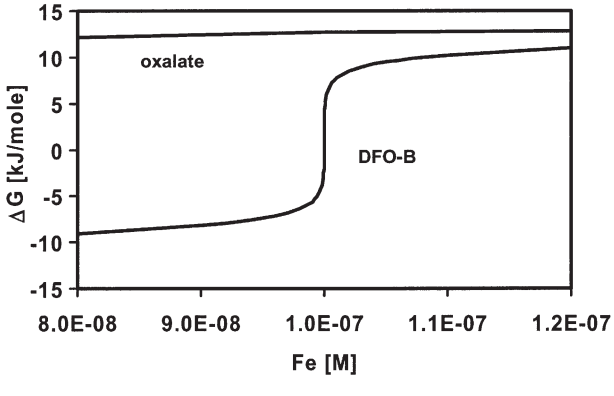

Figure 10. Calculated effect of 10^{-7} M DFO-B or 10^{-3} M oxalate on the solution saturation state with respect to goethite as a function of the soluble Fe(III) concentration. pH = 8.

Table 4. Thermodynamic formation constants, corrected to zero ionic strength with the Davies equation. T = 298.15 K.

Reaction	log K
$DFO\text{-}B^{3-} + H^+ = HDFO\text{-}B^{2-}$	11.45 [a]
$DFO\text{-}B^{3-} + 2\ H^+ = H_2DFO\text{-}B^-$	21.44 [a]
$DFO\text{-}B^{3-} + 3\ H^+ = H_3DFO\text{-}B$	30.62 [a]
$DFO\text{-}B^{3-} + 4\ H^+ = H_4DFO\text{-}B^+$	38.94 [a]
$HDFO\text{-}B^{2-} + Fe^{3+} = FeHDFO\text{-}B^+$	32.02 [a]
$FeDFO\text{-}B + H^+ = FeHDFO\text{-}B^+$	10.40 [a]
$FeHDFO\text{-}B^+ + H^+ = FeH_2DFO\text{-}B^{2+}$	0.68 [a]
$FeDFO\text{-}B + H^+ = FeHDFO\text{-}B^+$	10.40 [a]
$MugAc^{-4} + H^+ = HMugAc^{-3}$	17.98 [c]
$HMugAc^{-3} + H^+ = H_2MugAc^{-2}$	10.51 [c]
$H_2MugAc^{-2} + H^+ = H_3MugAc^-$	8.38 [c]
$H_3MugAc^- + H^+ = H_4MugAc$	3.45 [c]
$H_4MugAc + H^+ = H_5MugAc^+$	2.76 [b]
$H_5MugAc^+ + H^+ = H_6MugAc^{+2}$	2.17 [b]
$MugAc^{-4} + Fe^{3+} = FeMugAc^-$	35.74 [c]
$HMugAc^{-3} + Fe^{3+} = FeHMugAc$	19.69 [c]
$C_2O_4^{-2} + H^+ = HC_2O_4^-$	4.266 [a]
$HC_2O_4^{-2} + H^+ = H_2C_2O_4^-$	1.25 [a]
$C_2O_4^{-2} + Fe^{+3} = Fe(C_2O_4)^+$	9.33 [a]
$2\ C_2O_4^{-2} + Fe^{+3} = Fe(C_2O_4)_2^{2-}$	16.05 [a]
$3\ C_2O_4^{-2} + Fe^{+3} = Fe(C_2O_4)_3^{-3}$	20.28 [a]
$Fe^{3+} + OH^- = FeOH^{2+}$	11.81 [a]
$Fe^{3+} + 2\ OH^- = Fe(OH)_2^+$	23.4 [a]
$Fe^{3+} + 4\ OH^- = Fe(OH)_4^-$	34.4 [a]
$2\ Fe^{3+} + 2\ OH^- = Fe_2(OH)_2^{4+}$	25.14 [a]
$3\ Fe^{3+} + 4\ OH^- = Fe_3(OH)_4^{5+}$	49.7 [a]

[a] Martell et al., 1998.
[b] Sugiura et al., 1981.
[c] Murakami et al., 1989.

accelerate iron oxide dissolution by ligand-controlled dissolution mechanisms; 2) low free dissolved siderophore concentrations accelerate any ligand-controlled (or proton-promoted) dissolution mechanism by influencing the Gibbs free energy of the dissolution reaction.

The relative importance of both effects needs to be evaluated in light of the range of siderophore concentrations in natural systems. Assuming a dissolved hydroxamate siderophore concentration of 10^{-7} M in soils (Powell et al., 1980) and taking DFO-B as prototypical siderophore, the estimated surface excess of adsorbed siderophores on goethite surfaces is 7×10^{-10} [mole $\times$ m^{-2}] based on adsorption isotherm data published by Cheah et al., 2003. The calculated dissolution rate corresponding to this surface excess at pH = 5 is 1×10^{-11} [mole $\times$ $m^{-2} \times h^{-1}$], and therefore more then an order of magnitude slower then proton-promoted dissolution rates at the same pH (see Table 2). As noted earlier, siderophore concentrations in oligotrophic environments such as the marine system are even lower then the concentrations used for this calculation. However, oxalate and other low-molecular weight organic ligands are ubiquitous in soils and are usually found at micromolar to milimolar concentrations (Jones, 1998; Strobel, 2001). As pointed out by other authors (Casey and Holmen, 1996; Cocozza et al., 2002) hydroxamate ligands are surprisingly inefficient in accelerating goethite dissolution by ligand-controlled dissolution mechanisms. Therefore it seems likely that a central function of microbial siderophores in oligotrophic environments is to increase the solubility of iron oxides and to facilitate other dissolution mechanisms by lowering the solution saturation state. However, a full understanding of the role of siderophores in increasing iron oxide solubility and promoting dissolution in a natural system also requires the consideration of various processes and their rates such as exudation rates, uptake rates, and degradation rates, as well as loss of siderophores by adsorption on other mineral surfaces, partitioning into humic substance, and complexation of metals other then iron.

Conclusions and future challenges

Batch and steady state dissolution experiments have demonstrated that siderophores have a pronounced effect on the solubility and the dissolution kinetics of iron-bearing minerals. The relevance of these observations is validated by microbial culture experiments which indicate that microorganisms use the high affinity iron acquisition system to increase the bioavailability of iron from pure and substituted iron oxides of varying crystallinities and from iron-bearing silicates.

Siderophores promote iron oxide dissolution by a direct surface-controlled mechanism and by facilitating proton-promoted or other ligand-promoted dissolution mechanisms. The present knowledge of siderophore adsorption and siderophore-promoted dissolution mechanisms is based on observations involving a small number of siderophore analogs and siderophores. The best studied siderophore is DFO-B, owing to its commercial availability. The widespread use of DFO-B in solution chemical investigations, adsorption, and dissolution studies make it a useful reference siderophore. However, it is difficult to estimate to what extent DFO-B represents the full spectrum of the approximately 500 known siderophore structures. Investigations involving other siderophores usually requires the time consuming exercise of isolating them from iron-limited microbial cultures or plant exudates. Therefore it will be a challenging task to extend the range of dissolution studies to a few more "prototypical" siderophore structures.

Adsorption of siderophores at mineral surfaces is a necessary first step in surface-controlled siderophore-promoted dissolution. It also constitutes a loss of siderophore from the solution and therefore decreases the effect of siderophores on iron solubility. Both factors are important for understanding high affinity iron acquisition systems in soils and aquatic systems. Detailed studies on monohydroxamate adsorption and surface

speciation on goethite have been very useful for the interpretation of siderophore surface chemistry. However, direct spectroscopic observations of siderophore surface complexes are rare. Molecular level investigations of the local bonding environment of siderophores at mineral surfaces in combination with theoretical modeling are needed to close this important gap in our mechanistic understanding of siderophore adsorption and siderophore promoted dissolution.

In natural terrestrial and aquatic systems iron oxides are often coated with humic and fulvic acids, exopolysaccharides (biofilms), or biogenic low molecular weight organic acids. Inhibitory, competitive, or synergistic effects of such substances on siderophore-controlled iron acquisition need to be investigated.

Acknowledgments

Gratitude is expressed to Javiera Cervini-Silva and Garrison Sposito (University of California, Berkeley) for disclosing their newest research results, and to Scott Frazier for helpful comments and revisions of the manuscript. I thank Patricia Maurice and two anonymous reviewers whose comments greatly improved the manuscript.

References

Aagaard, P. and H. C. Helgeson, 1982. Thermodynamic and kinetic constraints on reaction-rates among minerals and aqueous solution. 1. Theoretical considerations. Am. J. Sci. **282:** 237–285.

Albrecht-Gary, A. M. and A. L. Crumbliss, 1998. Coordination chemistry of siderophores: Thermodynamics and kinetics of iron chelation and release. Metal Ions Biol. Sys. **35:** 239–327.

Ams, D. A., P. A. Maurice, L. E. Hersman and J. H. Forsythe, 2002. Siderophore production by an aerobic *Pseudomonas mendocina* bacterium in the presence of kaolinite. Chem. Geol. **188:** 161–170.

Bondietti, G., J. Sinniger and W. Stumm, 1993. The reactivity of Fe(III) (hydr)oxides – Effects of ligands in inhibiting the dissolution. Colloid. Surface A **79:** 157–167.

Bossier, P., M. Hofte and W. Verstraete, 1988. Ecological Significance of Siderophores in Soil. Adv. Microb. Ecol. **10:** 385–434.

Boudard, M. and G. Djega-Mariadassou, 1984. Kinetics of heterogeneous catalytic reactions. Princeton University Press, Princeton, pp. 222.

Boukhalfa, H. and A. L. Crumbliss, 2002. Chemical aspects of siderophore mediated iron transport. BioMetals **15:** 325–339.

Brown, G. E., V. E. Henrich, W. H. Casey, D. L. Clark, C. Eggleston, A. Felmy, D. W. Goodman, M. Gratzel, G. Maciel, M. I. McCarthy, K. H. Nealson, D. A. Sverjensky, M. F. Toney and J. M. Zachara, 1999. Metal oxide surfaces and their interactions with aqueous solutions and microbial organisms. Chem. Rev. **99:** 77–174.

Casey, W. H. and C. Ludwig, 1996. The mechanism of dissolution of oxide minerals. Nature **381:** 506–509.

Cervini-Silva, J. and G. Sposito, 2002. Steady-State Dissolution Kinetics of Aluminum-Goethite in the Presence of Desferrioxamine-B and Oxalate Ligands. Environ. Sci. Technol. **36:** 337–342.

Cervini-Silva, J. and G. Sposito, in preparation, a. Salt effect on goethite dissolution by desferrioxamine-B and oxalate ligands.

Cervini-Silva, J. and G. Sposito, in preparation, b. Adsorption of desferrioxamine-B and oxalate ligands on Al-goethites: implications for microbial dissolution processes.

Charlet, L., A. A. Manceau, 1992. X-ray absorption spectroscopic study of the sorption of Cr(III) at the oxide water interface. 2. Adsorption, coprecipitation, and surface precipitation on hydrous ferric-oxide. J. Colloid Interf. Sci. **148:** 443–458.

Cheah, S.-F., S. M. Kraemer, J. Cervini-Silva and G. Sposito, 2003. Steady state dissolution kinetics of goethite in the presence of Desferrioxamine-B and oxalate ligands: Implications for the microbial acquisition of iron. Chemical Geology **198:** 63–75.

Cocozza, C. and G. L. Ercolani, 1997. Produzione di siderofori e caratteristiche associate in pseudomonadi fluorescenti rizosferiche e non rizosferiche. Annali di microbiol. enzimol. **47:** 17–28.

Cocozza, C., C. C. G. Tsao, S. F. Cheah, S. M. Kraemer, K. N. Raymond, T. M. Miano and G. Sposito, 2002. Temperature dependence of goethite dissolution promoted by trihydroxamate siderophores. Geochim. Cosmochim. Acta **66:** 431–438.

Cornell, R. M., A. M. Posner and J. P. Quirk, 1976. Kinetics and mechanisms of the acid dissolution of goethite (α-FeOOH). J. Inorg. Nucl. Chem **38**: 563–567.

Cornell, R. M. and U. Schwertmann, 1993. The Iron oxides. Wiley-VCH, Weinheim, pp. 664.

Crumbliss, A. L. , 1990. Iron bioavailability and the coordination chemistry of hydroxamic acids. Coord. Chem. Rev. **105:** 155–179.

Crumbliss, A. L., 1991. Aqueous equilibrium and kinetic studies of iron siderophore and model siderophore complexes. In: G. Winkelmann (ed.), Handbook of microbial iron chelates, CRC Press, pp. 177–232.

Dinkelacker, B., V. Roemheld and H. Marschner, 1989. Citric acid excretion and precipitation of calcium citrate in the rhizosphere of white lupin. Plant Cell Environ. **12:** 285–292.

Fan, T. W.-M., A. N. Lane, J. Pedler, D. Crowley and R. M. Higashi, 1997. Comprehensive analysis of organic ligands in whole root exudates using nuclear magnetic resonance and gas chromatography-mass spectrometry. Anal. Biochem. **251:** 57–68.

Filius, J. D., T. Hiemstra and W. H. Van Riemsdijk, 1997. Adsorption of small weak organic acids on goethite: Modeling of mechanisms. J. Colloid Interf. Sci. **195:** 368–380.

Fung I. Y., S. K. Meyn and I. Tegen, 2000. Iron supply and demand in the upper ocean. Global Biogeochem. Cycles **14:** 281–295.

Furrer, G. and W. Stumm, 1986. The coordination chemistry of weathering. 1. Dissolution kinetics of delta-Al2O3 and BeO. Geochim. Cosmochim. Acta **50:** 1847–1860.

Fuerstenau, D. W. and M. Colic, 1999. Self-association and reverse hemimicelle formation at solid-water interfaces in dilute surfactant solutions. Colloids Surf. A. **146:** 33–47.

Gledhill, M. and C. M. G. van den Berg, 1994. Determination of complexation of iron(III) with natural organic complexing ligands in seawater using cathodic stripping voltammetry. Mar. Chem. **47:** 41–54.

Gledhill, M., C. M. G. van den Berg, R. F. Nolting and K. R. Timmermans, 1998. Variability in the speciation of iron in the northern North Sea. Mar. Chem. **59:** 283–300.

Gu, G. H., J. Schmitt, Z. Chen, L. Y. Liang and J. F. McCarthy, 1995. Adsorption and desorption of different organic-matter fractions on iron-oxide. Geochim. Cosmochim. Acta **59:** 219–229.

Hersman, L., T. Lloyd and G. Sposito, 1995. Siderophore-promoted dissolution of hematite. Geochim. Cosmochim. Acta **59:** 3327–3330.

Hersman, L., P. Maurice and G. Sposito, 1996. Iron acquisition from hydrous Fe(III)-oxides by an aerobic *Pseudomonas sp*. Chem. Geol. **132:** 25–31.

Hersman, L. E., J. H. Forsythe, L. O. Ticknor and P. A. Maurice, 2001. Growth of *Pseudomonas mendocina* on Fe(III) (hydr)Oxides. Appl. Environ. Microb. **67:** 4448–4453.

Hersman, L. E., 2000. The role of siderophores in iron oxide dissolution. IN: D. R Lovley (ed.) Environmental microbe-metal interactions, ASM, Washington, pp. 145–157.

Hiradate, S. and K. Inoue. 1998a. Interaction of mugineic acid with iron (hydr)oxides: Sulfate and phosphate influences. Soil Sci. Soc. Am. J. **62:** 159–165.

Hiradate, S. and K. Inoue, 1998b. Dissolution of iron form iron (hydr)oxides by mugineic acid. Soil Sci. Plant Nutr. **44:** 305–313.

Holmen, B. A. and W. H. Casey, 1996. Hydroxamate ligands, surface chemistry, and the mechanism of ligand-promoted dissolution of goethite [alpha-FeOOH(s)]. Geochim. Cosmochim. Acta **60:** 4403–4416.

Holmen, B. A., M. I. Tejedor and W. H. Casey, 1997. Hydroxamate complexes in solution and at the goethite-water interface: A cylindrical internal reflection Fourier transform infrared spectroscopy study. Langmuir **13:** 2197–2206.

Hou, Z., K. N. Raymond, B. O'Sullivan, T. W. Esker and T. Nishio, 1998. A preorganized siderophore: Thermodynamic and structural characterization of alcaligin and bisucaberin, microbial macrocyclic dihydroxamate chelating agents. Inor. Chem. **37:** 6630–6637.

Inoue, K., S. Hiradate and S. Takagi, 1993. Interaction of mugineic acid with synthetically produced iron oxides. Soil Sci. Soc. Am. J. **57:** 1254–1260.

Jones, D. L., 1998. Organic acids in the rhizosphere – a critical review. Plant Soil **205:** 25–44.

Kalinowski, B. E., L. J. Liermann, S. Givens and S. L. Brantley, 2000. Rates of bacteria-promoted solubilization of Fe from minerals: A review of problems and approaches. Chem. Geol. **169:** 357–370.

Parker, V. B. and I. L. Khodakovskii, 1995. Thermodynamic properties of the aqueous ions (2+ and 3+) of iron and the key compounds of iron. J. Phys. Chem. Ref. Data **24:** 1699–1745.

Kovacevic, D., I. Kobal and N. Kallay, 1998. Adsorption of organic acids on metal oxides. The umbrella effect. Croat. Chem. Acta **71:** 1139–1153.

Kummert, R. and W. Stumm,1980. The surface complexation of organic acids on hydrous gamma Al2O3. J. Collid. Interf. Sci. **75:** 373–385.

Kraemer, S. M., J. D. Xu, K. N. Raymond and G. Sposito, 2002. Adsorption of Pb(II) and Eu(III) by oxide minerals in the presence of natural and synthetic hydroxamate siderophores. Environ. Sci. Technol. **36:** 1287–1291.

Kraemer, S. M., S.-F. Cheah, R. Zapf, J. D. Xu, K. N. Raymond and G. Sposito, 1999. Effect of hydroxamate siderophores on Fe release and Pb(II) adsorption by goethite. Geochim. Cosmochim. Acta **63:** 3003–3008.

Kraemer, S. M. and J. G. Hering, 1997. Influence of solution saturation state on the kinetics of ligand-controlled dissolution of oxide phases. Geochim. Cosmochim. Acta **61:** 2855–2866.

Kraemer, S. M. and J. G. Hering, 1998. Influence of pH and competitive adsorption on the ligand-promoted dissolution of aluminum oxide. Environ. Sci. Technol. **32:** 2876–2882.

Lasaga, A. C., 1981. Transition state theory. Rev. Mineral. **8:** 135–169.

Langmuir, D., 1969. The Gibbs free energies of substances in the system Fe-O2-H2O-CO2 at 25 C. US Geological Survey Prof. Paper **650 B:** 180–184.

Leong, S. A. and G. Winkelmann, 1998. Molecular biology of iron transport in fungi. Metal Ions Biol. Syst. **35:** 147–186.

Liermann, L. J., B. E. Kalinowski, S. L. Brantley, J. G. Ferry, 2000. Role of bacterial siderophores in dissolution of hornblende. Geochim. Cosmochim. Acta **64:** 587–602.

Liermann, L. J., A. S. Barnes, B. E. Kalinowski, X. Y. Zhou and L. Susan, 2000. Microenvironments of pH in biofilms grown on dissolving silicate surfaces. Chem. Geol. **171:** 1–16.

Lindsay, W. L., 1979. Chemical equilibria in soils. Wiley Interscience, New York, 449 pp.

Loper, J. E. and M. D. Henkels, 1997. Availability of iron to *Pseudomonas fluorescens* in rhizosphere and bulk soil evaluated with an ice nucleation reporter gene. Appl. Environ. Microbiol. **63:** 99–105.

Ludwig, C., W. H. Casey and P. A. Rock, 1995. Prediction of ligand-promoted dissolution rates from the reactivities of aqueous complexes. Nature **375:** 44–47.

Margerum, D. W., G. R. Cayley, D. C. Weatherburn and G. K. Pagenkopf, 1978. Kinetics and mechanisms of complex formation and ligand exchange, In: A. E. Martell (ed.) Coordination Chemistry, Vol. 2, ACS Monograph **174**, ACS, Washington.

Martell, A. E., R. M. Smith and R. J. Motekaitis, 2001. NIST critically selected stability constants of metal complexes. NIST standard reference database **46**, Version 6.0, NIST Gaithersburg.

Martin, J. H. and S. E. Fitzwater, 1988. Iron-deficiency limits phytoplankton growth in the northeast Pacific subarctic. Nature **331:** 341–343.

Matzanke, B. F., G. Muller-Matzanke and K. N. Raymond, 1989. Siderophore mediated iron transport. In: T. M. Loehr (ed.), Iron carriers and proteins. VCH Publisher, New York pp. 1–121.

Maurice, P. A., Y. L. Lee and L. E. Hersman, 2000. Dissolution of Al-substituted goethites by an aerobic *Pseudomonas mendocina* var. bacteria. Geochim. Cosmochim. Acta **64:** 1363–1374.

Maurice, P. A., M. A. Vierkorn, L. E. Hersman and J. E. Fulghum, 2001a. Dissolution of well and poorly ordered kaolinites by an aerobic bacterium. Chem. Geol. **180:** 81–97.

Maurice, P. A., M. A. Vierkorn, L. E. Hersman, J. E. Fulghum and A. Ferryman, 2001b. Enhancement of kaolinite dissolution by an aerobic *Pseudomonas mendocina* bacterium. Geomicrobiol. J. **18:** 21–35.

Murakami, T., K. Ise, M. Hayakawa, S. Kamei and S. Takagi, 1989. Stabilities of metal-complexes of mugineic acids and their specific affinities for iron(III). Chem. Letters **12:** 2137–2140.

Neilands, J. B., 1957. Some aspects of microbial iron metabolism. Bacteriol. Rev. **21:** 101–111.

Neilands, J. B., K. Konopka, B. Schwyn, M. Coy, R.T. Francis, B.H. Paw and A. Bagg, 1987. Comparative biochemistry of microbial iron assimilation In: G. Winkelmann, D. Van der Helm, J. B. Neilands. (eds.), Iron Transport in Microbes, Plants and Animals, VCH, Weinheim, pp. 3–33.

Nelson, M., C. R. Cooper, D. E. Crowley, C. P. P. Reid and P. J. Szaniszlo, 1988. An Escherichia Coli Bioassay of Individual Siderophores in Soil. J. Plant Nutr. **11:** 915–924.

Neubauer, U., B. Nowack, G. Furrer and R. Schulin, 2000. Heavy metal sorption on clay minerals affected by the siderophore desferrioxamine B. Environm. Sci. Technol. **34:** 2749–2755.

Neubauer, U., G. Furrer and R. Schulin, 2002. Heavy metal sorption on soil minerals affected by the siderophore desferrioxamine B: the role of Fe(III) (hydr)oxides and dissolved Fe(III). Europ. J. Soil Sci. **53:** 45–55.

Nomoto, K., Y. Sugiur and S. Tagaki, 1987. Mugineic acids, studies on phytosiderophores. In: G. Winkelmann, D. Van der Helm, J.B. Neilands. (eds.), Iron Transport in Microbes, Plants and Animals, VCH, Weinheim, pp. 401–425.

Nowack, B. and L. Sigg, 1997. Dissolution of Fe(III)(hydr)oxides by metal-EDTA complexes. Geochim. Cosmochim. Acta **61:** 951–963.

Nowack, B., 2002. Environmental Chemistry of Aminopolycarboxylate Chelating Agents. Environ. Sci. Technol. **36:** 4009–4016.

Oelkers, E. H., 2001. General kinetic description of multioxide silicate mineral and glass dissolution. Geochim. Cosmochim. Acta **65:** 3703–3719.

Page, W. J. and M. Huyer, 1984. Derepression of the *Azotobacter vinelandii* siderophore system, using iron-containing minerals to limit iron repletion. J. Bacteriol. **158:** 496–502.

Powell, P. E., G. R. Cline, C. P. P. Reid and P. J. Szaniszlo, 1980. Occurrence of hydroxamate siderophore iron chelators in soils. Nature **287:** 833–834.

Powell, R. T. and J. R. Donat, 2001. Organic complexation and speciation of iron in the South and Equatorial Atlantic. Deep-Sea Res. II **48:** 2877–2893.

Raymond, K. N., G. Mueller and B. F. Matzanke, 1984. Complexation of iron by siderophores. A review of their solution and structural chemistry and biological function. Top. Curr. Chem. **123:** 49–102.

Römheld, V. and H. Marschner, 1986. Evidence for a specific uptake system for iorn phytosiderophores in roots of grasses. Plant. Physiol. **80:** 175–180.

Römheld V., 1991. The role of phytosiderophores in acquisition of iron and other micronutrients in graminaceous species: an ecological approach. Plant Soil **130:** 127–134.

Roosenberg, J. M., Y. M. Lin, Y. Lu, M. J. Miller, 2000. Studies and syntheses of siderophores, microbial iron chelators, and analogs as potential drug delivery agents. Curr. Med. Chem. **7**: 159–197.

Rosenberg, D. R. and P. A. Maurice, 2003. Siderophore adsorption to and dissolution of kaolinite at pH 3 to 7 and 22 degrees C. Geochim. Cosmochim. Acta **67:** 223–229.

Rue, E. L. and K. W. Bruland, 1997. The role of organic complexation on ambient iron chemistry in the equatorial Pacific Ocean and the response of a mesoscale iron addition experiment. Limnol Oceanogr. **42:** 901–910.

Scheffer, F. and P. Schachtschabel, 2002. Lehrbuch der Bodenkunde. (Ed.: H.-P. Blume) Spektrum, Heidelberg, 593 pp.

Schindler, P., W. Michaelis and W. Feitknecht, 1963. Loeslichkeitsprodukte von Metalloxiden und –hydroxiden. 8. Die Loeslichkeit gealterter Eisen(III)-hydroxid-Faellungen. Helv. Chim. Acta **46:** 444–451.

Simpson, S. L., K. J. Powell and S. Sjoberg, 2000. Pyrocatechol violet complexation at the boehmite-water interface. J. Colloid. Interf. Sci. **229:** 568–574.

Spasojević, I., S. K. Amstrong, T. J. Brickman and A. L. Crumbliss, 1999. Electrochemical behavior of the Fe(III) complexes of the cyclic hydroxamate siderophores alcaligin and desferrioxamine E. Inorg. Chem **38:** 449–454.

Strobel, B. W., 2001. Influence of vegetation on low-molecular-weight carboxylic acids in soil solution – a review. Geoderma **99:** 169–198.

Sugiura, Y., H. Tanaka, Y. Mino, T. Ishida, N. Ota, M. Inoue, K. Nomoto, H. Yoshioka and T. Takemoto, 1981. Structure, properties, and transport mechanism of iron(III) complex of mugineic acid, a possible phytosiderophore. J. Am. Chem. Soc. **103:** 6979–6982.

Sverjensky, D. A., 1994. Zero-point-of-charge prediction from crystal-chemistry and salvation theory. Geochim. Cosmochim. Acta **58:** 3123–3129.

Takagi, S. I., 1976. Naturally occurring iron-chelating compounds in oat-root and rice-root washings. 1. Activity measurement and preliminary characterization. Soil Sci. Plant Nutr. **22:** 423–433.

Telford, J. R. and K. N. Raymond, 1996. Molecular recognition: Receptors for cationic guests. In: J. Atwood, J. E. D Davies, D. D. MacNicol and F. Voegtle (eds.), Comprehensive macromolecular chemistry, Elsevier Science, Oxford, pp. 245–266.

Temkin, M. I., 1971. The kinetics of steady-state complex reactions. Intern. Chem. Eng. **11:** 709–717.

Trolard, F. and Y. Tardy, 1987. The stabilities of gibbsite, boehmite, aluminous goethites and aluminous hematites in bauxites, ferricretes and laterites as a function of water activity, temperature and particle size. Geochim. Cosmochim. Acta **51:** 945–957.

van den Berg, C. M. G., 1995. Evidence for organic complexation of iron in seawater. Mar. Chem. **50:** 139–157.

Vasudevan, D. and A. T. Stone, 1996. Adsorption of catechols, 2-aminophenols, and 1,2-phenylenediamines at the metal (hydr)oxide/water interface: Effect of ring substituents on the adsorption onto TiO2. Environm. Sci. Technol. **30:** 1604–1613.

Vasudevan, D. and A. T. Stone, 1998. Adsorption of 4-nitrocatechol, 4-nitro-2-aminophenol, and 4-nitro-1,2-phenylenediamine at the metal (hydr)oxide/water interface: Effect of metal (hydr)oxide properties. J. Colloid Interf. Sci. **202:** 1–19.

Voelker, C. and D. A. Wolf-Gladrow, 1999. Physical limits on iron uptake mediated by siderophore or surface reductases. Mar. Chem. **65:** 227–244.

Watteau, F. and J. Berthelin, 1994. Microbial dissolution of iron and aluminum from soil minerals – efficiency and specificity of hydroxamate siderophores compared to aliphatic acids. Europ. J. Soil Biol. **30:** 1–9.

Wehrli, B., E. Wieland and G. Furrer, 1990. Chemical mechanics in the dissolution kinetics of minerals; the aspect of active sites. Aquatic Sciences **1:** 3–31.

Wieland, W., B. Wehrli and W. Stumm, 1988. The coordination chemistry of weathering: III. A generalization on the dissolution rates of minerals. Geochim. Cosmochim. Acta **52:** 1969–1981.

Wilhelm, S. W., 1995. Ecology of iron-limited cyanobacteria: A review of physiological responses and implications for aquatic systems. Aquatic Microb. Ecol. **9:** 295–303.

Wilson, T. R. S., 1975. In: J. P. Riley and G. Skirrow (eds.) Chemical Oceanography, Academic Press, London, pp. 365–414.

Winkelmann, G., 1992. Structures and functions of fungal siderophores containing hydroxamate and complexone type iron binding ligands. Mycol. Res. **96:** 529–534.

Witter, A. E. and G. W. Luther, 1998. Variation in Fe-organic complexation with depth in the Northwestern Atlantic Ocean as determined using a kinetic approach. Mar. Chem. **62:** 241–258.

Wu, J. F. and G. W. Luther, 1995. Complexation of Fe(III) by natural organic-ligands in the northwest Atlantic-ocean by a competitive ligand equilibration method and a kinetic approach. Mar. Chem. **50:** 159–177.

Yoshida, T., K. Hayashi and H. Ohmoto, 2002. Dissolution of iron hydroxides by marine bacterial siderophore. Chem. Geol. **184:** 1–9.

Zhuang, G., R. A. Duce and D. R. Kester, 1990. The Dissolution of Atmospheric Iron in Surface Seawater of the Open Ocean. J. Geophys. Res. **95:** 16207–16216.

Zinder, B., G. Furrer and W. Stumm, 1986. The coordination chemistry of weathering. 2. Dissolution of Fe(III)oxides. Geochim. Cosmochim. Acta **50:** 1861–1869.